Technical Note

23

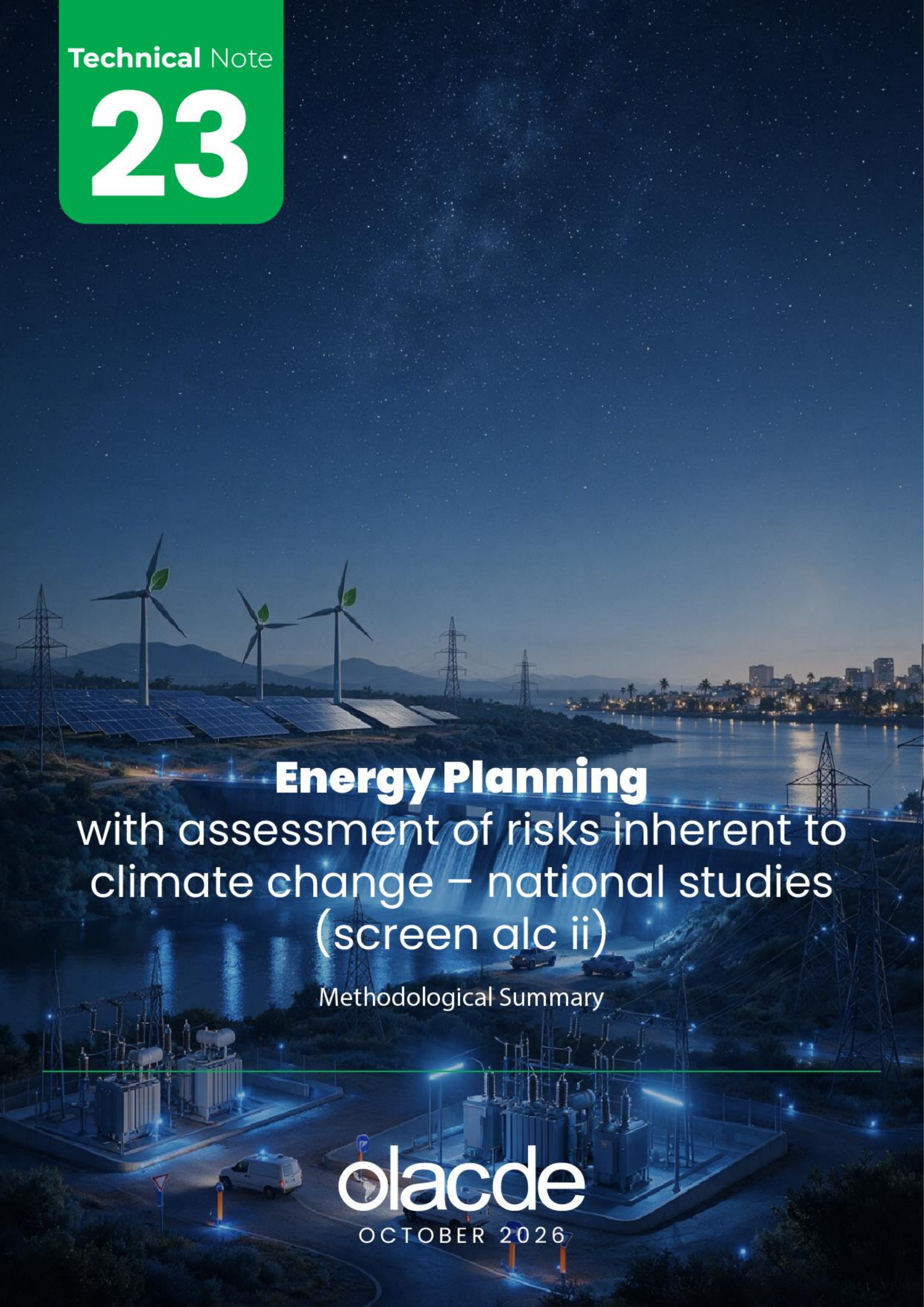

Energy Planning

with assessment of risks inherent to climate change – national studies (screen alc ii)

Methodological Summary

olacde

OCTOBER 2026

olacde Technical Note 23

olacde

aecid
Agencia Española
de Cooperación Internacional
para el Desarrollo

TECHNICAL NOTE No. 23

ENERGY PLANNING WITH ASSESSMENT OF RISKS INHERENT TO CLIMATE CHANGE – NATIONAL STUDIES (SCREEN ALC II)

Methodological Summary

With Technical Assistance from:

tecnalia
MEMBER OF BASQUE RESEARCH
& TECHNOLOGY ALLIANCE

olacde
Technical Note 23

This document was prepared under the direction of

Latin American and Caribbean Energy Organization (OLACDE)

Andrés Rebolledo Smitmans

Executive Secretary

Fitzgerald Cantero Piali

Director of Studies, Projects and Information

Developed by

Fabio García Lucero

OLACDE Specialist

Jorge Paz

TECNALIA Specialist

Quito, Ecuador

October 2026

Content

1. INTRODUCTION 1

2. GENERAL CONSIDERATIONS ON THE METHODOLOGY FOR ASSESSING CLIMATE CHANGE-RELATED RISKS 2

3. CLIMATE SCENARIOS CONSIDERED IN THE STUDY 2

4. ASSESSMENT OF CLIMATE CHANGE IMPACTS ON HYDROELECTRIC POWER GENERATION 5

4.1. Characterization of Climate-Related Hazards to Hydroelectric Systems 5

4.2. Representation of the Hydroelectric System 5

4.3. Hydropower Model 7

4.4. Hydrological Model Calibration 9

5. ASSESSMENT OF CLIMATE CHANGE IMPACTS ON SOLAR PHOTOVOLTAIC POWER GENERATION 11

5.1. Characterization of Climate-Related Hazards to Photovoltaic Systems 11

5.2. Climatic Variables Affecting Photovoltaic Power Generation 14

5.3 Databases Used 13

5.4 Extraction of the ERA5 Grid Point 14

5.5. Evaluation of Climate Change Impacts on Photovoltaic Power 15

6. ASSESSMENT OF CLIMATE CHANGE IMPACTS ON WIND POWER GENERATION 20

6.1. Characterization of Climate-Related Hazards to Wind Power Systems 20

6.2. Climatic Variables Affecting Wind Power Generation 21

6.3. Data Sources Used 22

6.4. Assessment of Climate Change Impacts on Wind Power Generation 22

7. ASSESSMENT OF CLIMATE CHANGE IMPACTS ON TRANSMISSION AND DISTRIBUTION NETWORKS 24

7.1. Characterization of Climate-Related Hazards to Transmission and Distribution (T&D) Systems 24

7.2. Methodological Approach to Climate Risk Assessment 27

8. ASSESSMENT OF CLIMATE CHANGE IMPACTS ON COASTAL FACILITIES 27

8.1. Characterization of Climate-Related Hazards to Wind Power Systems 27

8.2. Concepts Related to Sea Level Height 28

8.3. Assessment of the Impacts of Sea Level Rise 28

8.4. Data Used in the Analysis 29

8.5. Methodology for Storm Characterization 29

9. GENERAL CONCLUSIONS ON THE METHODOLOGIES APPLIED IN THE STUDY: 30

10. REFERENCES 31

List of Figures

Figure 1. General Procedure for Assessing Climate Change-Related Risks 2
Figure 2. Representative Concentration Pathways (RCPs) 3
Figure 3. Example of a Hydropower Simulation Model 6
Figure 4. Example of a Model Configuration for Analyzing a Hydroelectric System Consisting of a Power Plant with a Reservoir and Two Upstream Streamflow Gauging Stations 7
Figure 5. Typical Efficiency Curves for Different Types of Turbines. 8
Figure 6. Example of a Comparison Between Observed and Modeled Values. 10
Figure 7. Example of a Comparison Between Observed and Modeled Values 11
Figure 8. Methodology for Comparing Historical and Projected Power Generation 17
Figure 9. Example of average energy generation by decade. The point represents the mean annual energy generation for the decade, while the bars indicate the annual minimum and maximum. The recurring sawtooth pattern every 30 years is an artifact of the repeated ERA5 sequence, rather than a climate signal 19
Figure 10. Seasonal Change by 30-Year Window. 20
Figure 11. Power Curve Values for a Representative Wind Turbine 23
Figure 12. Comparison Between Static and Dynamic Maximum Current Ratings 25

List of Tables

Table 1 Relationship Between Climate Scenarios 5
Table 2 CORDEX Models Considered 14
Table 3: Experiments Considered in the Analysis and Data Series Used. 18
Table 4 Excerpt from the Table Relating Energy Infrastructure Components to Threshold Values and Potential Impacts 27

Energy Planning with Assessment of Climate Change-Related Risk

Methodological summary.

1. INTRODUCTION

Although the energy sector in Latin America and the Caribbean (LAC) accounts for only a small share of global greenhouse gas (GHG) emissions, contributing approximately 5%, its infrastructure can be highly vulnerable to the impacts of climate change. These impacts can compromise both the physical integrity of energy facilities and their operational performance and productivity, jeopardizing the energy security and economic stability of countries in the region.

The potential impacts of climate change on energy infrastructure may result from extreme weather events or unusual variations in climatic conditions, such as floods, droughts, unusually high sea levels, and strong wind gusts, as well as changes in energy demand patterns.

In this context, the Latin American and Caribbean Energy Organization (OLACDE), with financial support from the Spanish Agency for International Development Cooperation (AECID) and technical assistance from the Tecnalia Foundation, has carried out the project "Energy Planning with Assessment of Climate Change-Related Risk – National Studies (Screen LAC II)."

The objective of the project was to assess the vulnerability, potential impacts, and risks associated with climate change affecting major existing and planned energy infrastructure in five Latin American and Caribbean countries: Honduras, Panama, Paraguay, the Dominican Republic, and Uruguay. The project also proposed adaptation measures that could be incorporated into the planning, expansion, and operation of their respective energy systems, with an assessment horizon extending to 2050.

Each beneficiary country selected the energy sector facilities that, based on its national criteria and priorities, could be most vulnerable to climate change. The assets considered in the studies included hydroelectric, solar photovoltaic, and wind power plants, electricity transmission and distribution systems, refineries, and ethanol production plants.

Given the diversity of energy infrastructure analyzed within the framework of the project, OLACDE considered it appropriate to share with the Latin American and Caribbean community the knowledge gained and the experience acquired through the application of analytical methodologies across various case studies. However, due to the confidential nature of the quantitative results for each specific facility, this document focuses on presenting the methodological approaches applied and the experiences gained from their implementation, without disclosing the individual quantitative results of the facilities assessed. These results are available in individual country reports, which are accessible exclusively to the focal points designated for the project by the energy authorities of each beneficiary country.

2. GENERAL CONSIDERATIONS ON THE METHODOLOGY FOR ASSESSING CLIMATE CHANGE-RELATED RISKS

The methodology proposed for the study encompasses the analysis of each of the components that constitute the term "**RISK**." Following the recommendations of the Intergovernmental Panel on Climate Change (IPCC), risk is defined by the relationship between climate-related hazards, the exposure of systems to these hazards, and their vulnerability.

Within this conceptual framework, the methodology is divided into four stages:

1. Characterization of climate change hazards.
2. Analysis of the energy sector's exposure and vulnerability to climate change.
3. Assessment of potential impacts.
4. Preliminary risk assessment.

Figure 1. General Procedure for Assessing Climate Change-Related Risks

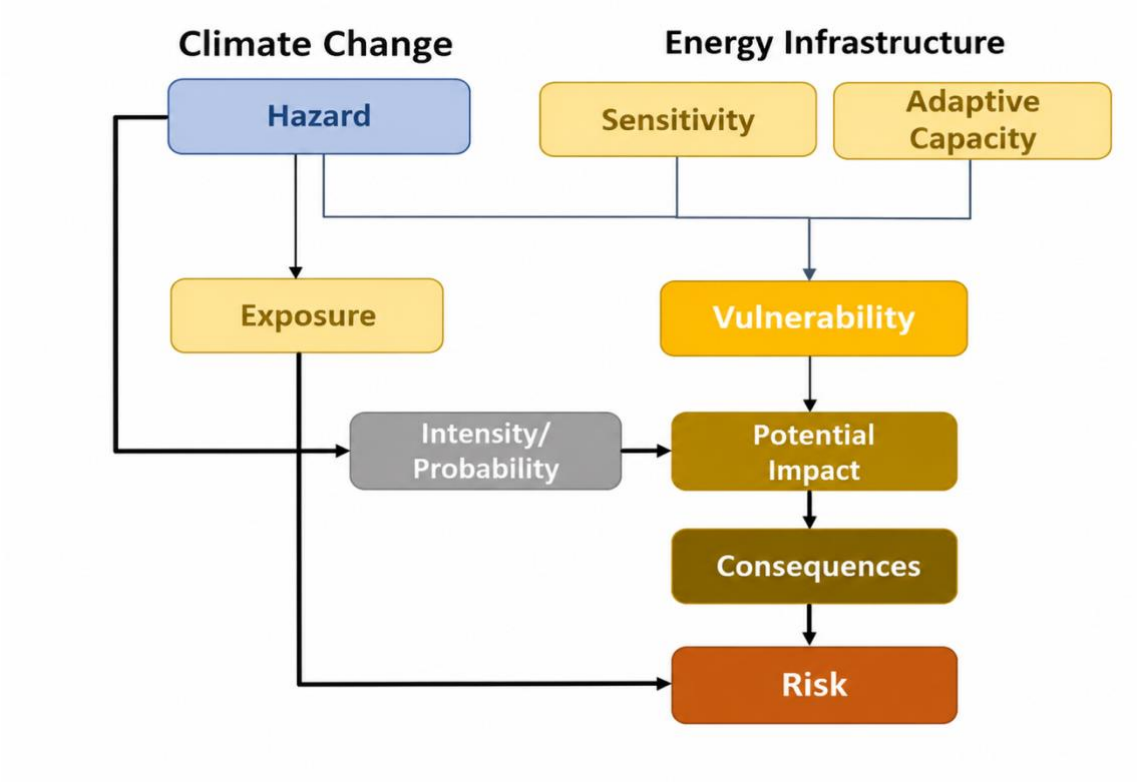

3. CLIMATE SCENARIOS CONSIDERED IN THE STUDY

Climate scenarios are tools used to describe possible future climate developments based on consistent sets of assumptions about key drivers, such as demographics, the economy, technological innovation, governance, and lifestyles. According to the IPCC, these scenarios

represent plausible descriptions of the future and make it possible to analyze how current decisions and trends could influence future climate conditions.

The definition of climate scenarios depends largely on the selected time horizon. Climate is characterized by atmospheric properties whose statistical values are considered representative over extended periods of time. Therefore, it is necessary to select intervals that are sufficiently long to capture interannual and intra-annual variability, while remaining appropriate for characterizing the conditions of each period analyzed. Typically, periods of 20 to 30 years are used to represent both historical climate conditions and different future time horizons. The selection of these intervals directly influences the accuracy of the results, as longer-term projections generally involve greater uncertainty. Furthermore, the longer the operational lifespan of a project, the broader the range of scenarios that should be considered to assess potential climate changes.

The development of climate scenarios evolves alongside advances in climate models. Based on different assumptions regarding future greenhouse gas emissions and other factors affecting the Earth's energy balance, these models generate simulations that allow for the exploration of different climate trajectories. In this way, climate scenarios provide relevant information for planning, risk assessment, and climate change adaptation.

Among the scenarios used, the Representative Concentration Pathways (RCPs) stand out, classified according to the projected level of radiative forcing by 2100. The RCP2.6 scenario represents a stringent mitigation pathway aimed at keeping emissions low. The RCP4.5 and RCP6.0 scenarios correspond to intermediate levels of radiative forcing stabilization. Meanwhile, the RCP8.5 scenario assumes very high emissions, associated with sustained emissions growth throughout the 21st century.

In conclusion, the selection of climate scenarios and time horizons makes it possible to assess different potential climate trajectories, taking into account both the uncertainty associated with climate projections and the specific needs of each project. See Figure 2.

Figure 2. Representative Concentration Pathways (RCPs)

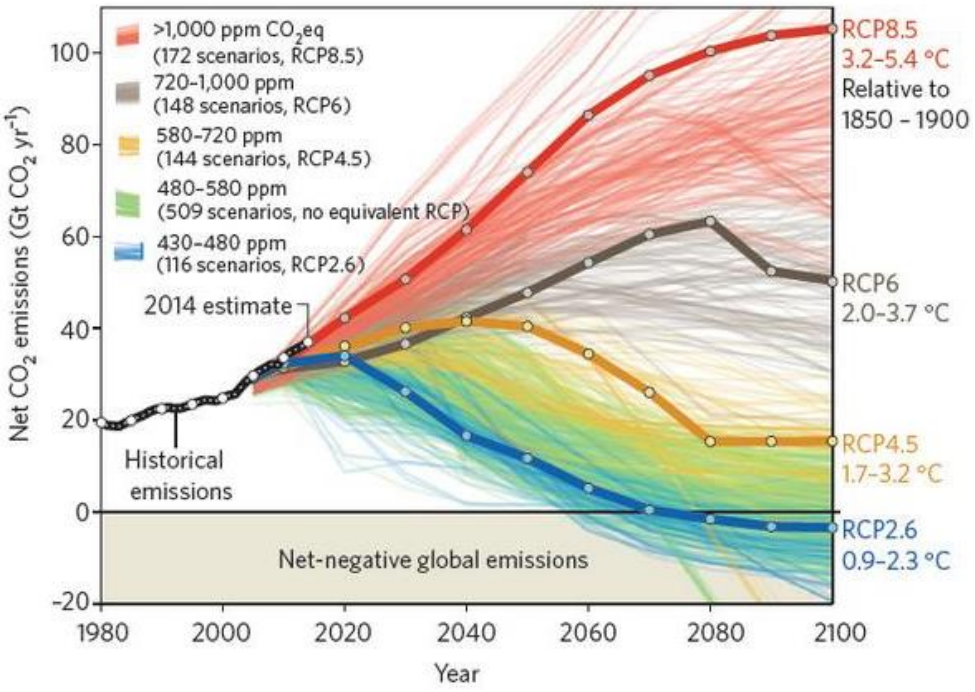

Source: Neil Craik, University of Waterloo

The Shared Socioeconomic Pathways (SSPs) describe possible future social and economic conditions that influence greenhouse gas emissions and the capacity for climate change mitigation and adaptation. Five main pathways are identified: SSP1, focused on sustainability; SSP2, representing a middle-of-the-road development pathway; SSP3, characterized by regional rivalry; SSP4, associated with inequality; and SSP5, based on fossil fuel-intensive development.

Furthermore, Global Warming Levels (GWLs) classify climate projections according to the projected increase in global mean temperature during the 21st century. These range from scenarios that limit warming to 1.5°C to those in which warming exceeds 4°C.

To assess the impacts of climate change, the Shared Socioeconomic Pathways (SSPs) are combined with the Representative Concentration Pathways (RCPs). However, the possible combinations depend on the consistency between the socioeconomic conditions assumed and the associated emissions levels. This integration gives rise to nine potential scenarios, five of which are particularly noteworthy: SSP1-1.9, SSP1-2.6, SSP2-4.5, SSP3-7.0, and SSP5-8.5.

These scenarios represent a wide range of plausible futures, from low-emission pathways consistent with limited warming to high-emission scenarios in which global warming could exceed 4°C by 2100. Their relationship with global warming levels makes it possible to analyze potential climate impacts and assess the relevance of mitigation commitments and strategies. Together, they serve as essential tools for understanding climate uncertainty and guiding planning and adaptation efforts in response to future changes. See Table 1.

Table 1 Relationship Between Climate Scenarios [1]

Category description	GHG emissions scenarios (SSPx-y*) in WGI & WGII	RCPy** in WGI & WGII
limit warming to 1.5°C (>50%) with no or limited overshoot	Very low (SSP1-1.9)	
return warming to 1.5°C (>50%) after a high overshoot		
limit warming to 2°C (>67%)	Low (SSP1-2.6)	RCP2.6
limit warming to 2°C (>50%)		
limit warming to 2.5°C (>50%)		
limit warming to 3°C (>50%)	Intermediate (SSP2-4.5)	RCP 4.5
limit warming to 4°C (>50%)	High (SSP3-7.0)	
exceed warming of 4°C (>50%)	Very high (SSP5-8.5)	RCP 8.5

The selection of scenarios (time horizons, emissions scenarios, etc.), spatial resolution, and models to be used will depend in part on the availability and quality of information in climate databases. Existing knowledge gaps often require qualitative approaches and the formulation of assumptions. As a general principle, multiple future scenarios and a historical reference scenario are used to enable comparisons.

For the purposes of this study, the RCP4.5 scenario (representing moderate climate change) and the RCP8.5 scenario (representing a more pessimistic and severe climate change trajectory) have been selected, with a projection horizon extending to 2050.

4. ASSESSMENT OF CLIMATE CHANGE IMPACTS ON HYDROELECTRIC POWER GENERATION

4.1. Characterization of Climate-Related Hazards to Hydroelectric Systems

In this step, the potential hazards to which the hydroelectric system is exposed are identified and selected, and all available information, including historical data and projections, is collected.

To this end, climate indicators are defined to estimate the potential impact of climate change on hydroelectric infrastructure. This assessment is based on changes in available water flows, which will affect the power plant's electricity generation.

Based on available historical time series of daily inflows, covering both the period before dam construction and the period during its operation, the hydropower model is calibrated and the reference scenario is established.

Regarding future climate conditions, projections of changes in water flow were obtained using data from the **AQUEDUCT** database. AQUEDUCT is a data platform developed and managed by the World Resources Institute (WRI) that provides information and maps on water-related risks worldwide. Among other information, AQUEDUCT offers projections of water availability and

[1] Climate Change 2023: Synthesis Report. Contribution of Working Groups I, II and III to the Sixth Assessment Report of the Intergovernmental Panel on Climate Change [Core Writing Team, H. Lee and J. Romero (eds.)]. (2023). IPCC, Geneva, Switzerland, pp. 35-115, doi: 10.59327/IPCC/AR6-9789291691647. https://www.ipcc.ch/report/ar6/syr/downloads/report/IPCC_AR6_SYR_LongerReport.pdf

helps users understand long-term trends in water stress. It is primarily a prioritization tool and should therefore be complemented by more detailed analyses at the local and regional levels. Essentially, AQUEDUCT combines geospatial and climate models with statistical methods to translate global hydrological data into indicators and aggregated scores that can support decision-making and the development of water management strategies.

4.2. Representation of the Hydroelectric System

Based on the information gathered on the hydroelectric systems to be analyzed and the associated climate hazards, the methodology to be applied in the study was established. This methodology was developed by Tecnalia, drawing on experience gained from various projects assessing the impacts of climate change on hydroelectric power generation and its application to different systems, and was adapted to the specific needs of the present project. It consists of several successive stages:

- Development of a hydropower model to simulate the operation of reservoirs, canals, power plants, and other components of the hydroelectric system.
- Calibration of the hydropower model by comparing its results with available historical data on water flows, reservoir storage volumes, electricity generation, and other relevant parameters.
- Incorporation of climate projections of water flows into the hydropower simulation model to assess changes in water flows, hydroelectric power generation, and other parameters under study.
- Evaluation of the results obtained under climate projections and comparison with the baseline scenario.

In general, the tool that will allow addressing this sequence is a hydro-energy simulation model whose input data are the flows of the main channel at the beginning of a hydroelectric system and, where appropriate, the tributaries that feed it, and whose main outputs are the flows that circulate through each of its sections, pipelines, rivers, etc. and the energy generated by the different uses that make up the hydroelectric system.

Figure 3. Example of a Hydropower Simulation Model

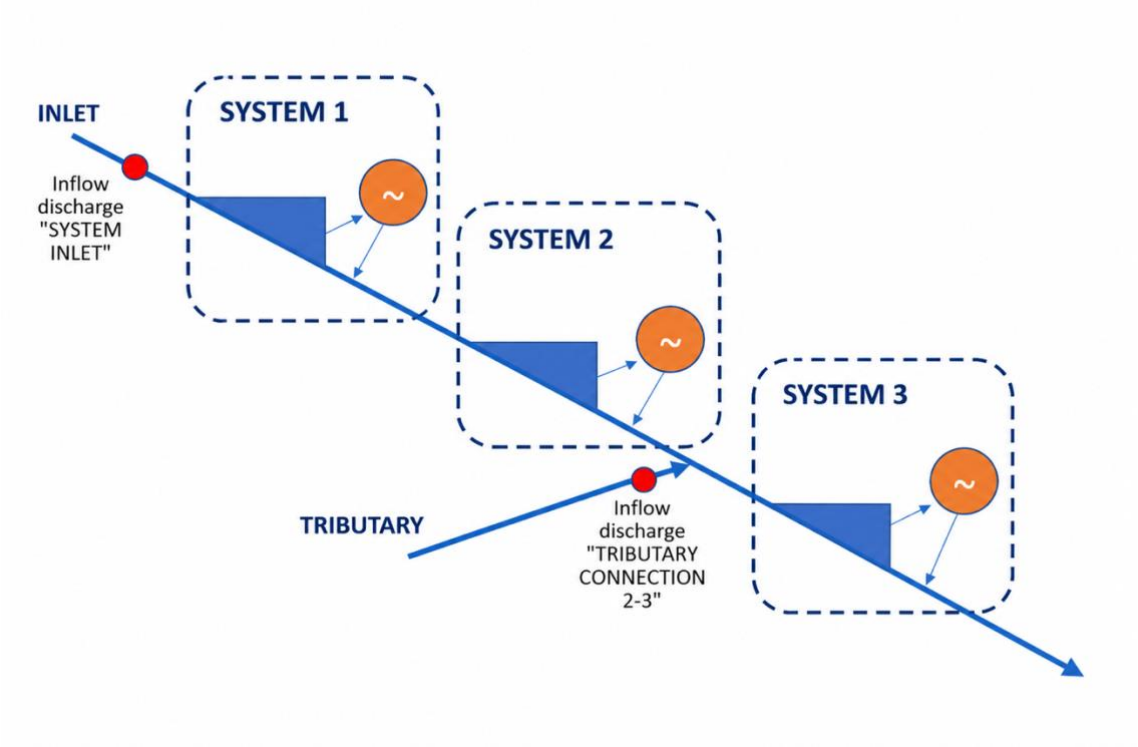

4.3. Hydropower Model

The development of the hydropower model involves creating a set of components that, when integrated and combined, make it possible to simulate any configuration of hydropower plants or hydroelectric systems.

Figure 4. Example of a Model Configuration for Analyzing a Hydroelectric System Consisting of a Power Plant with a Reservoir and Two Upstream Streamflow Gauging Stations

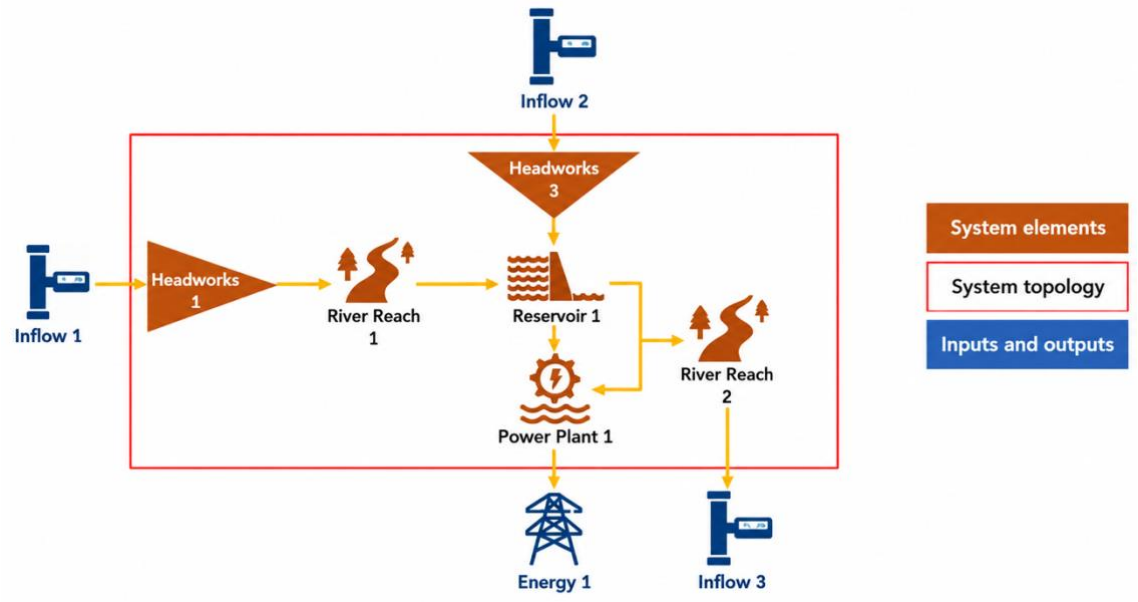

The rules governing reservoir operation can be summarized as follows:

- Reservoir operation always prioritizes meeting the environmental flow requirement, which is generally released through the turbines.
- The main outflow from the reservoir is determined at each time step based on the inflow, the stored water volume, and the reservoir operating rules. In the absence of more detailed operational information, the following assumptions are made:
    - When the reservoir is full, the outflow is equal to the inflow, while ensuring compliance with the environmental flow requirement. The outflow does not exceed the sum of the maximum spillway discharge capacity and the authorized water withdrawal rate.
    - When the reservoir water level is below the minimum level required for turbine operation, the outflow is minimized and limited to the amount necessary to meet the environmental flow requirement.
    - In all other cases, the maximum available flow is released without exceeding the authorized water withdrawal rate.
- Based on this outflow, it is assumed that the maximum possible flow is directed through the turbines, provided that the power plant's operating limits are not exceeded and the reservoir water level remains above the minimum level required for turbine operation. Due to the existing transmission line constraint, the flow through the turbines is limited, with the turbines operating in parallel at below their rated power output.
- The remaining flow (total outflow minus the flow passing through the turbines) is discharged through the spillway.

The hydropower plant, in turn, receives the flow directed through the turbines and produces electricity as its output. For hydropower plants that use water released from a reservoir, the energy generated is calculated by multiplying the inflow to the turbines (turbined flow) by the plant's energy conversion coefficient (kWh/m³). This coefficient is determined based on the available information, as follows:

- Based on the elevation–efficiency–volume curves as a function of the reservoir's usable storage volume.
- Based on measured power plant operating data (electricity generation and turbine flow).

In cases where specific information on the hydropower facility is unavailable, the “typical” turbine efficiency curves shown in Figure 5 are used, applying them to the authorized flow rates of each power plant. To enable their application across the full range of flow rates, polynomial trendlines are fitted to each curve.

Figure 5. Typical Efficiency Curves for Different Types of Turbines.

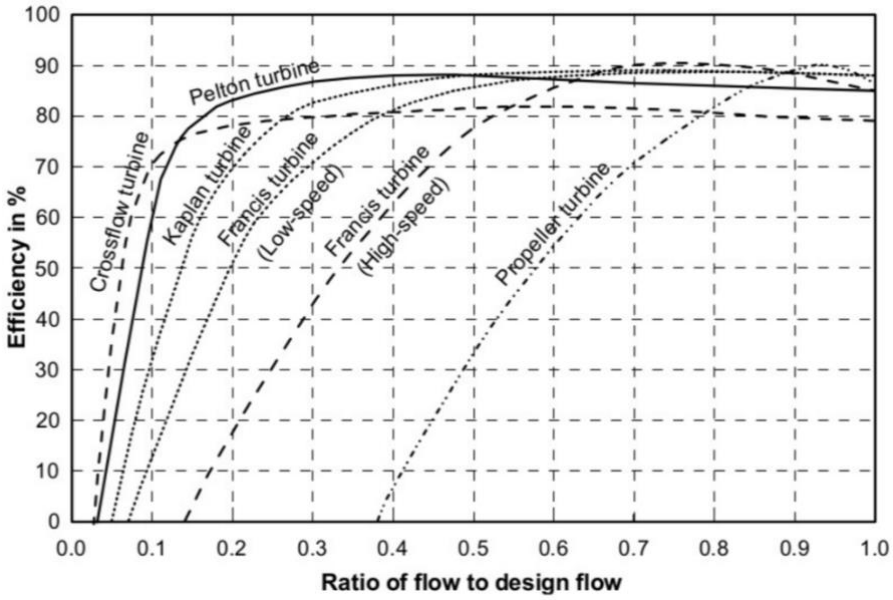

To provide the necessary inputs for this model, detailed information on the hydroelectric system under study is used. In general, the different stages of the analysis require different types of information.

The development and calibration of the model require:

- An inventory of the dams and reservoirs that make up the hydroelectric system.
- Data on the system's topology, including its configuration, specific characteristics, interconnections between infrastructure components, operating limits, and other relevant parameters.
- Historical data covering several years (preferably 10 or more) on:
    - Characteristics of reservoirs and hydropower plants:
        - Maximum, usable, and dead storage volumes.
        - Spillway discharge capacity.
        - Elevation-efficiency-volume curves.
        - Authorized flow rate for each power plant and/or flow data for individual turbines and the number of turbines.
        - Number and type of turbines in run-of-river hydropower plants.
        - Hydraulic head (elevation difference).
    - Daily available usable storage volume in each reservoir.
    - Daily spilled, turbined, and diverted flow rates at each dam and hydropower plant.
    - Daily environmental flow requirements for each river channel or river reach.
    - Reservoir operating rules under alert conditions (spillway operation rules, etc.).

Once the model has been calibrated, simulating any given period requires the following information:

- Historical data:

- Daily inflow to the model during the study period (measured at the upstream gauging station located at the starting point of the system).
- Daily flow rates (during the study period) for all known water inflows and outflows throughout the system (including measurements at reservoir and hydropower facility inlets, tributaries, interbasin water transfers, etc.).
- Usable storage volume of the reservoirs within the system on the first day of the study period (Day 1, at the beginning of the day).

- Climate projections:
  - The same data, but accounting for the effects of climate change. This information can be obtained from calibrated hydrological models driven by climate projections. Within the framework of the project, streamflow projections were generated as described in the section "Characterization of Climate-Related Hazards."

4.4. Hydrological Model Calibration

To **calibrate the simulation model** representing the hydropower system, historical observed data provided by the power plant operators are used, such as a multiyear time series of daily flow measurements recorded at the gauging station upstream of the reservoir.

Using the flow data and technical information describing the infrastructure, the model is run to estimate daily reservoir outflows, flow rates passing through the power plant's turbines, and electricity generation. Comparing these simulated time series with observed values (actual data provided by the operator) makes it possible to assess the accuracy of the model.

Error! Reference source not found. illustrates an example of these comparisons, highlighting the differences between observed (actual) and modeled values.

Figure 2. Example of a Comparison Between Observed and Modeled Values.

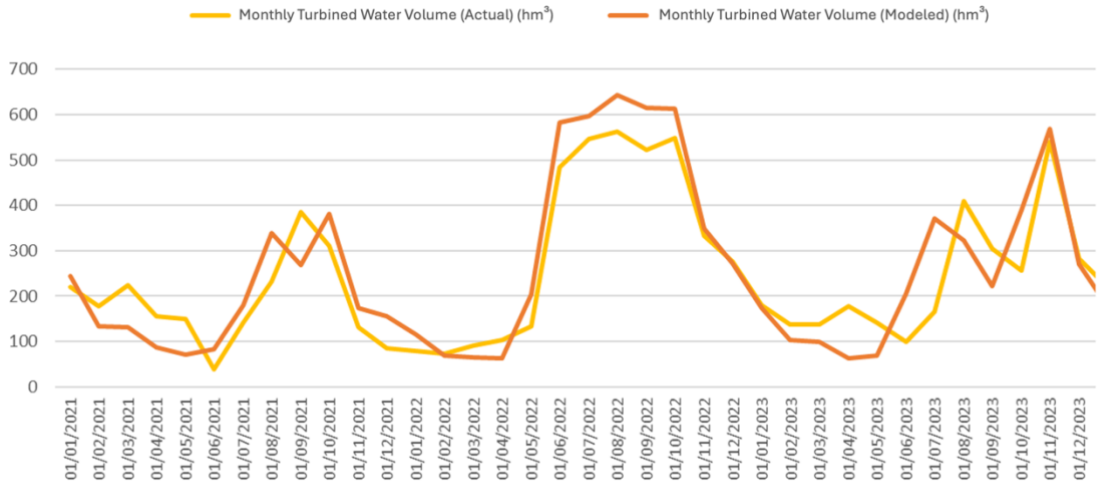

By running the hydropower model using the inflow data, the following outputs are obtained: the water flows that are extracted daily from the reservoir, as well as turbine flows in the plant and the energy generated.

Figure 7 provides an example of results normalized relative to the historical average.

Figure 3. Example of a Comparison Between Observed and Modeled Values.

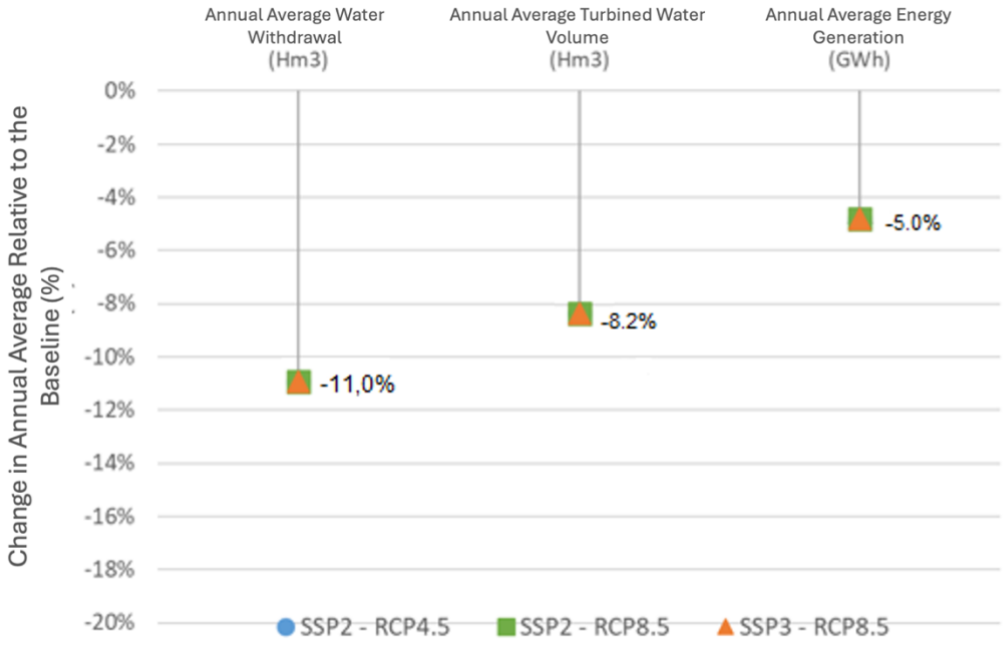

It should be noted that the impacts of climate change on hydropower plants do not necessarily result in reduced inflows and electricity generation. In some cases, depending on the geographical location of the power plant, climate change may lead to an increase in these values relative to the reference scenario.

5. ASSESSMENT OF CLIMATE CHANGE IMPACTS ON SOLAR PHOTOVOLTAIC POWER GENERATION

5.1. Characterization of Climate-Related Hazards to Photovoltaic Systems

The analysis was conducted using a quantitative methodological approach to assess the potential impacts of climate change on solar photovoltaic power generation. To this end, the main climatic variables affecting the efficiency of solar panels were considered: surface downwelling shortwave radiation (RSDS), ambient temperature (Tm), and wind speed (WS).

Given that these variables may be affected by climate change, they were analyzed under different greenhouse gas (GHG) emissions scenarios. Specifically:

- Current climate conditions were obtained from the ERA5 atmospheric reanalysis dataset of the European Centre for Medium-Range Weather Forecasts (ECMWF), available through the Climate Data Store (CDS) of the Copernicus Climate Change Service (C3S), which provides high-resolution data based on observations and numerical models.
- Future projections of these variables were obtained from the regional climate models of the CORDEX project, which make it possible to assess projected changes throughout the 21st century under different greenhouse gas (GHG) emissions scenarios.

The methodology is structured into three main sections:

- Climatic variables affecting photovoltaic power generation: This section describes the three key variables that determine the efficiency and performance of solar panels (temperature, solar radiation, and wind speed). For each variable, its influence on photovoltaic power generation and its potential evolution under future climate scenarios are analyzed.
- Databases used: Data sources are used to characterize present and future climate conditions, including historical datasets and projections from regional climate models.
- Calculation of photovoltaic power generation potential: This section describes the methodology used to estimate photovoltaic power generation potential based on climatic variables. It presents the equations used to calculate photovoltaic cell temperature and the performance ratio, as well as how these are incorporated into the estimation of electricity generation.

5.2. Climatic Variables Affecting Photovoltaic Power Generation

The power generation potential of a photovoltaic installation depends primarily on the amount of available solar energy (surface downwelling shortwave radiation, RSDS). However, other factors also influence the efficiency of photovoltaic cells, including the physical characteristics of the installation, its age, shading, soiling, electrical losses, and, particularly, climatic conditions.

In the context of climate change, three variables are particularly relevant, as they may undergo significant changes under different emissions scenarios:

- Ambient temperature (Tm)
- Wind speed (VWS)
- Surface downwelling shortwave radiation (RSDS)

Given that the risk assessment covers the entire century, all other variables are assumed to remain constant. This implies that, throughout the study period, the power plant is assumed to maintain similar efficiency levels across its components, with no changes in electrical losses, shading conditions, or other relevant factors.

Temperature and Its Impact on Photovoltaic Efficiency

Although higher solar radiation generally leads to greater photovoltaic power generation, an increase in ambient temperature has a negative effect on the efficiency of solar modules above 25°C. The efficiency of photovoltaic cells begins to decline beyond this temperature, and previous studies indicate that this reduction ranges from 0.3% to 0.5% for each additional degree Celsius (Energías Renovables, 2015). This effect may be even more pronounced due to the photovoltaic cell temperature (Tcell), which is typically higher than the ambient temperature because of heat accumulation within the modules.

Wind Speed and Heat Dissipation

Wind speed plays a key role in the thermal regulation of solar modules. Moderate increases in wind speed can help cool photovoltaic cells by dissipating some of the accumulated heat and mitigating the negative effects of rising temperatures. However, this cooling effect becomes significant only when wind speed reaches certain minimum thresholds.

Since the values analyzed in the study correspond to daily averages, they do not capture the effects of occasional wind gusts, which could provide more effective cooling than that reflected in the daily averages. To assess this phenomenon more accurately, historical observations collected on-site at a higher temporal resolution would be required.

Although the wind speed values presented correspond to daily averages aggregated into decadal averages of annual values, the calculation of photovoltaic power generation potential is based on the original daily data. This approach captures seasonal and intra-annual variability in wind speed, providing a more accurate representation of natural fluctuations throughout the year.

Surface Downwelling Solar Radiation and Energy Availability

Together, these three climatic factors interact and determine the performance of photovoltaic installations. Although an increase in solar radiation may partially offset the losses caused by rising temperatures, photovoltaic power generation is more severely affected when solar radiation decreases and temperatures increase. Furthermore, wind speed can only partially mitigate these effects if the increase is sufficiently significant. Therefore, the impact of climate change on photovoltaic power generation depends on the combined influence of these factors, highlighting the importance of analyzing them under different emissions scenarios.

5.3. Databases Used

To assess the impact of climate change on photovoltaic power generation, two main sources of climate data were used. First, reanalysis data were employed to characterize current climate conditions. Second, projections from regional climate models were used to estimate future changes in key climatic variables.

Reference Period 1991-2020 (ERA5)

Reference climate data were obtained from the ERA5 reanalysis dataset, developed by the Copernicus Climate Change Service (C3S). This dataset provides global climate information based on the assimilation of observations into numerical models, with a spatial resolution of approximately 0.25° × 0.25° (~31 km × 31 km at the equator) and a daily temporal resolution. For this study, the 1991–2020 period was used as the reference period for analyzing observed climate conditions.

The variables extracted include air temperature at 2 meters (*2m_temperature*), expressed in Kelvin and subsequently converted to degrees Celsius; wind speed at 10 meters, calculated from the zonal (10m_u_component_of_wind) and meridional (*10m_v_component_of_wind*) wind components, expressed in meters per second (m/s); and surface downwelling solar radiation (*surface_solar_radiation_downwards*), originally expressed in joules per square meter (J/m²) and converted to watts per square meter (W/m²) by dividing by 86,400 seconds.

Regional Climate Model Projections for Estimating Future Changes in Climatic Variables (CORDEX)

To assess future changes in these variables under different climate change scenarios, projections from the Coordinated Regional Climate Downscaling Experiment (CORDEX) were used,

specifically for the South American domain. These regional climate simulations have a horizontal resolution of 0.44° × 0.44° (~50 km × 50 km) and a daily temporal resolution.

The CORDEX models include historical data from 1950 to 2005 and future projections from 2006 to 2100. To construct a historical data series equivalent to the ERA5 reference period (1991–2020), CORDEX historical values for 1991–2005 were combined with model projections for 2006–2020 under both scenarios. Specifically, future projections were analyzed under the two greenhouse gas emissions scenarios considered in the study (RCP4.5 and RCP8.5).

The variables used in the projections include air temperature at 2 meters (*2m_air_temperature*), expressed in Kelvin and converted to degrees Celsius; wind speed at 10 meters (*10m_wind_speed*), expressed in meters per second (m/s); and surface downwelling solar radiation (surface_solar_radiation_downwards), expressed in watts per square meter (W/m²).

To ensure an adequate representation of the uncertainty associated with different climate models, multiple combinations of Global Climate Models (GCMs) and Regional Climate Models (RCMs) were used. In this study, based on criteria of consistency and data availability (requiring that all selected models have data available for all periods under both scenarios), the following model combinations were selected for the South American region:

Table 2. CORDEX Models Considered[2]

Global Model (GCM)	Regional Model (RCM)	Ensemble Member
NRM-CERFACS-CNRM-CM5	SMHI-RCA4	r1i1p1
ICHEC-EC-EARTH	SMHI-RCA4	r12i1p1
IPSL-CM5A-MR	SMHI-RCA4	r1i1p1
MOHC-HADGEM2-ES	SMHI-RCA4	r1i1p1
CCCMA-CANESM2	SMHI-RCA4	r1i1p1
CSIRO-QCCCE-CSIRO-MK3-6-0	SMHI-RCA4	r1i1p1
NOAA-GFDL-ESM2M	SMHI-RCA4	r1i1p1
MIROC-MIROC5	SMHI-RCA4	r1i1p1
MPI-M-MPI-ESM-LR	MPI-CSC-REMO2009	r1i1p1
MPI-M-MPI-ESM-LR	SMHI-RCA4	r1i1p1
NCC-NORESM1-M	SMHI-RCA4	r1i1p1

5.4. Generation of Bias-Corrected Climate Variable Projections

Extraction of the ERA5 Grid Point

The assessment of photovoltaic power generation potential is based on the ERA5 reanalysis dataset, used as an observational reference to characterize historical climate conditions at the solar power plant site. The grid cell closest to the plant's location was selected, avoiding spatial interpolation. Hourly data for the 1991–2024 period were extracted for three main variables: air temperature at two meters, surface downwelling shortwave radiation, and horizontal wind

[2] Climate Change 2023: Synthesis Report. Contribution of Working Groups I, II and III to the Sixth Assessment Report of the Intergovernmental Panel on Climate Change [Core Writing Team, H. Lee and J. Romero (eds.)]. (2023). IPCC, Geneva, Switzerland, pp. 35-115, doi: 10.59327/IPCC/AR6-9789291691647. https://www.ipcc.ch/report/ar6/syr/downloads/report/IPCC_AR6_SYR_LongerReport.pdf

components at ten meters (u10 and v10). These variables characterize the climatic resources at the site and provide the basis for applying future climate projections.

Since the photovoltaic power generation model operates at a daily temporal resolution, the hourly data were aggregated according to the physical characteristics of each variable. Daily temperature was calculated as the average of the 24 hourly observations, while solar radiation was obtained by summing the hourly values and expressing the result as accumulated energy in Wh/m^2 per day. For wind, speed was calculated from the horizontal components as the square root of the sum of their squares, maintaining hourly resolution throughout the processing.

To ensure the quality of the field data, outlier detection and correction procedures were applied. For solar radiation, the Modified Z-Score method was used with a centered 30-day moving window and a threshold of 1.5; anomalous values were replaced using linear temporal interpolation. For temperature, the method was applied separately by hour of the day and month of the year, using a threshold of 4.5 to identify anomalies without excluding plausible climatic extremes.

Subsequently, systematic biases in ERA5 were corrected by comparing the reanalysis data with valid observations from the power plant's meteorological station. Adjustments were calculated on a monthly basis, applying an additive correction to temperature and a multiplicative correction to solar radiation.

To account for climate change, the monthly Delta Mapping methodology was implemented using 11 pairs of global and regional climate models from CORDEX South America. The RCP4.5 and RCP8.5 scenarios were analyzed for the periods 2011–2040, 2041–2070, and 2071–2100, using 2006–2020 as the reference period. Temperature anomalies were calculated as absolute differences, while relative change factors were used for solar radiation and wind speed.

Finally, the adjustments were applied to the historical ERA5 time series, preserving their daily and interannual variability while incorporating the projected climate change signals. The resulting time series make it possible to assess photovoltaic power generation potential under different future climate change scenarios.

5.5. Assessment of Climate Change Impacts on Photovoltaic Power Generation

Calculation of Photovoltaic Power Generation Potential

Photovoltaic power generation potential was calculated following the methodology proposed by Jerez et al. (2015), which has been applied in numerous subsequent studies, including Park et al. (2020). This methodology makes it possible to assess the impact of climate change on photovoltaic power generation by combining key climatic variables, such as air temperature, wind speed, and surface downwelling shortwave radiation.

Different photovoltaic technologies exhibit varying responses under the same climatic conditions (Crook, 2011). In this analysis, a general formulation was used based on the relationship between available solar radiation and system efficiency, which is influenced by photovoltaic cell temperature. The main equation used to calculate photovoltaic power generation potential is expressed as follows:

$$PV_{pot}(t) = P_R(t) * \frac{RSDS\ (t)}{RSDS_{STC}}$$

where:

$PV_{pot}(t)$ is the photovoltaic power generation potential at a given time *t*, expressed as a quantity relating electricity generation to the rated capacity of the installations.

$RSDS\ (t)$ is the surface downwelling solar radiation.

$RSDS_{STC} = 1000\ W/m^2$ is the solar irradiance under Standard Test Conditions (STC)[3].

$P_R(t)$ is the performance ratio of the photovoltaic system, defined as:

$$P_R(t) = 1 + \gamma[T_{cell}(t) - T_{STC}]$$

where:

$T_{cell}(t)$ is the temperature inside the photovoltaic cell at a given time t.

$T_{STC} = 25°C$ is the temperature under Standard Test Conditions (STC).

$\gamma = -0.005°C^{-1}$ is a coefficient representing the typical temperature response of monocrystalline silicon panels[4].

The photovoltaic cell temperature, $T_{cell}(t)$, is calculated based on ambient temperature, solar radiation, and wind speed, following the formulation proposed by Chenni et al. (2007):

$$T_{cell}(t) = c_1 + c_2 TAS(t) + c_3\ RSDS(t) + c_4\ WS(t)$$

where:

$TAS(t)$ is the near-surface air temperature at a given time t.

$RSDS(t)$ is the surface downwelling solar radiation at a given time *t.*

$WS(t)$ is the wind speed at a given time *t.*

The coefficients were also taken from Chenni et al. (2007), with the following values:

$$c_1 = 4.3°C$$

$$c_2 = 0.943\ (adimensional)$$

$$c_3 = 0.028°C\ m^2/W$$

$$c_4 = -1.528°C\ s/m$$

The resulting photovoltaic power generation potential is expressed as a dimensionless value (or, alternatively, as a fraction of the theoretical peak power), indicating the relative performance of

[3] *Clarification on units: The solar radiation time series is generated in Section 3.2.4.2 as accumulated daily energy, expressed in Wh/m²/day. Before being used in this equation, the time series is converted to average daily irradiance in W/m² by dividing by the 24 hours in a day. With RSDS(t) expressed in W/m², the ratio RSDS(t)/RSDS_STC is strictly dimensionless (W/m² divided by W/m²), consistent with the formulation proposed by Jerez et al. (2015).*

[4] The coefficient provided by Jerez et al. applies to monocrystalline panels, whereas the information collected indicates that the plant uses polycrystalline panels. Nevertheless, this coefficient is applied because no equivalent coefficient for polycrystalline panels has been identified in the scientific literature. Polycrystalline panels may exhibit slightly greater sensitivity to temperature.

the photovoltaic system compared with standard conditions (based on a performance ratio of 1, corresponding to the standard temperature of 25°C and an irradiance of 1,000 W/m² under Standard Test Conditions, STC).

The methodological approach employed makes it possible to assess the influence of climate change on photovoltaic power generation throughout the 21st century, considering the combined effects of rising temperatures, variations in solar radiation, and the moderating effect of wind speed.

Calculation of Theoretical Energy Generation and Comparison with Actual Generation

After calculating PVpot for the historical time series, theoretical power generation is determined by multiplying PVpot by the plant's rated capacity.

Subsequently, a relationship is established between the gross electricity generation measured on-site over the entire time series and the theoretical generation calculated for the same period. This relationship is calculated as the ratio of the sum of measured energy generation to the sum of projected energy generation over the same period, as shown below:

$$f = \frac{\sum P_m}{\sum P_C}$$

Where P_m is the electricity generation measured on-site over a given period, and P_c is the generation calculated from PVpot using the formula proposed by Jerez et al. (2015).

The same factor is applied to future theoretical generation time series, making it possible to quantify the combined effects of climatic variables on photovoltaic power generation and directly compare historical generation with projected generation (Figure 8).

Figure 8. Methodology for Comparing Historical and Projected Power Generation.

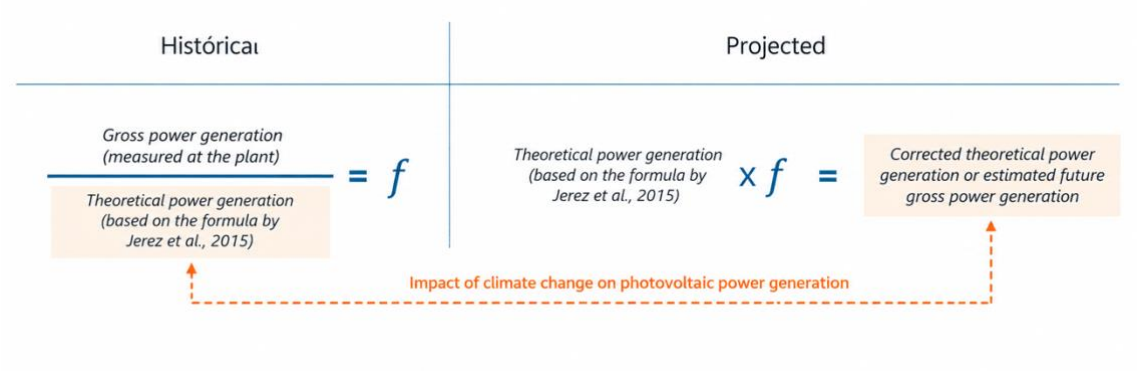

Calculation of the CORDEX Model Ensemble

The study employs a multimodel ensemble approach to integrate CORDEX climate simulations for the South American domain, with the aim of reducing uncertainty and obtaining more representative climate projections. The methodology involves averaging the available realizations for each GCM-RCM combination, integrating the results from different regional

climate models associated with each global climate model, and finally averaging across all global climate models. In addition, minimum and maximum values are calculated to represent the spread and uncertainty of the projections. The results are stored separately for the RCP4.5 and RCP8.5 emissions scenarios and are used to assess photovoltaic power generation potential.

To analyze long-term climate and energy trends, annual and seasonal averages are calculated using 30-year moving windows. The variables considered include air temperature, wind speed, surface downwelling solar radiation, photovoltaic cell temperature, and the system performance ratio. For photovoltaic power generation, annual values are summed for each decade, and their average is calculated. Maximum and minimum values are also determined to characterize the variability of the variables during each period.

The seasonal analysis considers four periods: December–February (DJF), March–May (MAM), June–August (JJA), and September–November (SON). For each season, average photovoltaic power generation over the 30-year window and its daily average are calculated, allowing comparisons of generation across seasons and an assessment of intra-annual variability.

Photovoltaic power generation depends on the interaction between solar radiation, temperature, and wind speed. An increase in solar radiation can partially offset losses caused by high temperatures, while a decrease in solar radiation combined with rising temperatures can significantly reduce power generation. Wind can partially mitigate these effects by cooling the photovoltaic modules.

Finally, the study proposes assessing the individual contribution of each climatic variable to the projected change in photovoltaic power generation potential through five separate PVpot calculations for each 30-year period, varying the projected variables while keeping the remaining variables at their historical reference values.

Table 2: Experiments Considered in the Analysis and Data Series Used.

Experiment	Temperature	Radiation	Wind
$PVpot_{base}$	historical	historical	historical
$PVpot_{T}$	projected	historical	historical
$PVpot_{RSDS}$	historical	projected	historical
$PVpot_{V}$	historical	historical	projected
$PVpot_{total}$	projected	projected	projected

In each experiment, the approximately 11,000 daily PVpot values for the period are averaged. The contribution of each variable is defined as the percentage change in its corresponding experiment relative to the PVpot_base reference:

$$cambio_X = \frac{PVpot_X - PVpot_{base}}{PVpot_{base}} \; x \; 100$$

The total change corresponds to the $PVpot_{total}$ experiment relative to the same reference.

The three individual contributions do not sum exactly to the total change; the residual is explicitly reported as an interaction term:

$$interacción = cambio_{TOTAL} - (cambio_T + cambio_{RSDS} + cambio_v)$$

This residual does not represent a numerical error or an a posteriori adjustment, but rather a direct consequence of the nonlinear relationship between PVpot and its input variables. Solar radiation enters the formulation twice —as an energy resource in the numerator (RSDS / RSDS_STC) and through cell temperature, which governs the thermal performance of the module—, simultaneously modifying solar radiation and temperature does not produce the same effect as modifying them separately and summing their individual contributions.

Decadal Analysis

The calculation process described above produces decadal projections, such as those shown in Figure 9. It should be clarified that the future trajectories do not generate new meteorological conditions for each year. Instead, they are based on the observed 30-year sequence (ERA5, 1991–2020), which is repeatedly reused for future periods, with the climate change signal corresponding to each scenario superimposed on it. In practice, this means that the same sequence of years reappears every 30 years.

Figure 4. Example of average energy generation by decade. The point represents the mean annual energy generation for the decade, while the bars indicate the annual minimum and maximum. The recurring sawtooth pattern every 30 years is an artifact of the repeated ERA5 sequence, rather than a climate signal.

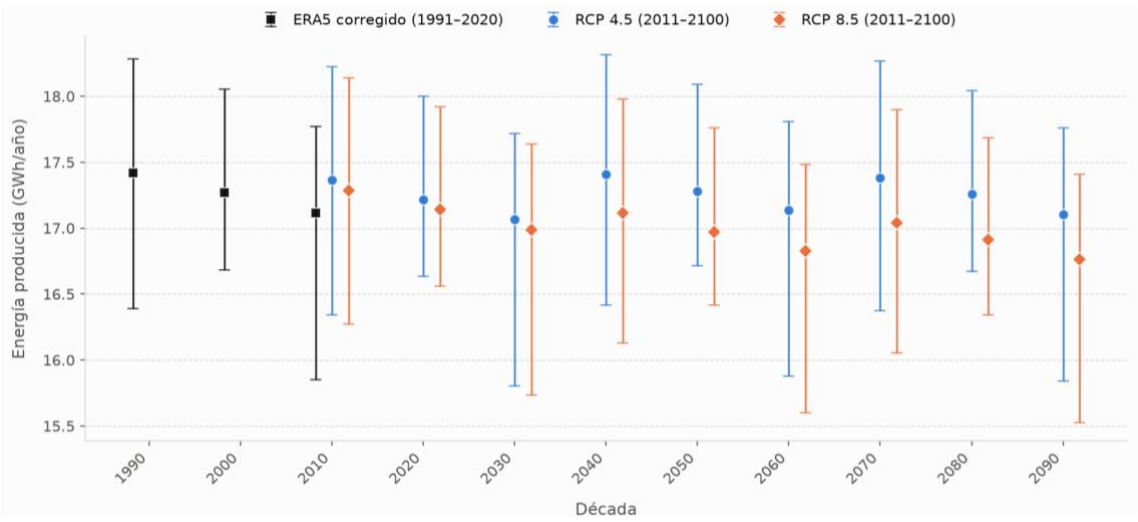

Seasonal Analysis

The values presented thus far correspond to annual averages. However, photovoltaic power generation potential fluctuates throughout the year due to seasonal variations in temperature, solar radiation, and wind speed. Therefore, seasonal projections can also be obtained, as illustrated in the example shown in Figure 10.

Figure 5. Seasonal Change by 30-Year Window

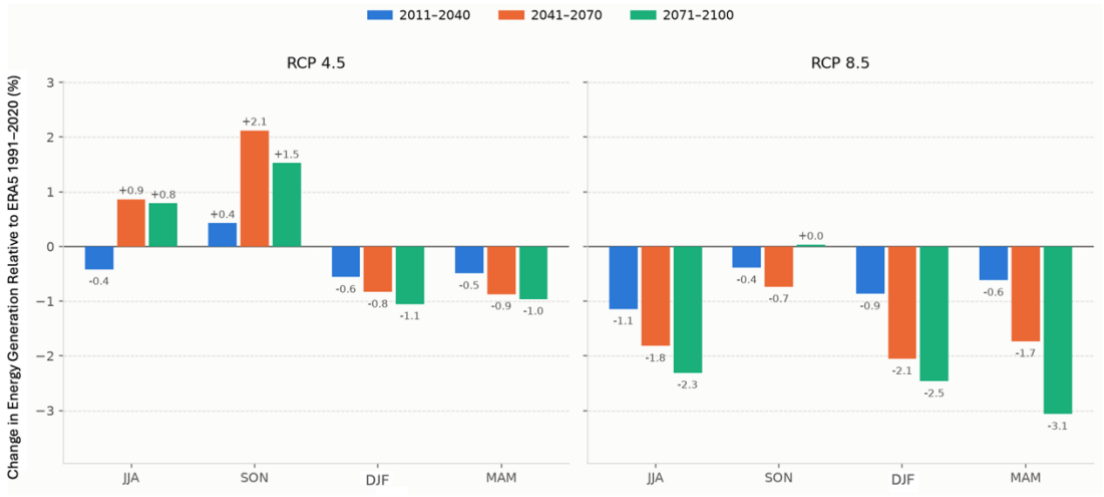

6. ASSESSMENT OF CLIMATE CHANGE IMPACTS ON WIND POWER GENERATION

6.1. Characterization of Climate-Related Hazards to Wind Power Systems

The analysis was conducted using a quantitative methodological approach to assess the potential impacts of climate change on wind power generation. To this end, the main climatic variables affecting wind turbine efficiency were considered: wind speed (WS) and air temperature (TAS).

Given that these variables may be affected by climate change, they were analyzed under different greenhouse gas (GHG) emissions scenarios. Specifically:

Current climate conditions were obtained from the ERA5 reanalysis dataset available through the Climate Data Store (CDS) of the European Centre for Medium-Range Weather Forecasts (ECMWF), which provides high-resolution data based on observations and numerical models.

Future projections of these variables were obtained from the regional climate models of the CORDEX project, which make it possible to assess projected changes throughout the 21st century under different greenhouse gas (GHG) emissions scenarios.

The methodology is structured into three main sections:

Climatic variables affecting wind power generation: The two key variables that determine wind turbine efficiency and performance (WS and TAS) are described. For each variable, its influence on wind power generation and its potential evolution under future climate scenarios are analyzed.

Data sources used: The information sources used to characterize present and future climate conditions are described in detail, including datasets for the historical period and future projections from regional climate models.

Calculation of Wind Power Generation Potential: The methodology used to estimate wind power generation potential based on climatic variables is described.

6.2. Climatic Variables Affecting Wind Power Generation

The power generation potential of a wind power installation depends primarily on the speed of the main available resource (wind, WS). However, other factors also influence wind turbine efficiency, including the characteristics of the installed turbines, their age, terrain conditions, pollution, electrical losses, and, particularly, climatic conditions.

In the context of climate change, two variables are particularly relevant, as they may undergo significant changes under different emissions scenarios:

- Wind speed
- Ambient temperature

Wind Speed and Aerodynamic Efficiency

Wind speed is the most significant factor influencing wind power generation, as the power generated by a turbine is proportional to wind speed. Small increases in wind speed can result in significant increases in energy generation. However, the relationship between wind speed and wind power generation is nonlinear, as turbines have a cut-in wind speed, a rated wind speed, and a cut-out wind speed.

- **Cut-in wind speed:** The minimum wind speed at which the turbine begins generating electricity (generally 3 m/s).
- **Rated wind speed:** The wind speed at which the turbine reaches its maximum power output (11 m/s for the power curve of the selected representative wind turbine model).
- **Cut-out wind speed:** The wind speed at which the turbine shuts down to prevent structural damage (21 m/s for the power curve of the selected representative wind turbine model).

Under climate change scenarios, changes in average wind speed may affect wind power generation in different ways. If wind speed decreases, the number of hours during which turbines operate above their cut-in wind speed could decline, reducing annual energy generation. Conversely, increases in average wind speed could improve performance if wind speeds remain within the optimal operating range.

Since the values analyzed in this study correspond to daily averages, they do not capture the effects of short-duration wind gusts, which could result in higher actual power generation than that estimated using daily averages. A more accurate assessment of this phenomenon would require historical *in situ* observations with higher temporal resolution.

Although the wind speed values presented correspond to daily averages aggregated into decadal averages of annual values, the calculation of wind power generation potential is based on the original daily values. This makes it possible to capture seasonal variability in wind speed, providing a more accurate representation of the natural fluctuations in wind resources throughout the year.

Temperature and Its Impact on Wind Power Generation Efficiency

Although wind speed is the primary determinant of wind power generation, ambient temperature also plays an important role, mainly through its influence on air density. The power extracted by a wind turbine is directly related to air density, which decreases as temperature

increases. This means that, under otherwise identical conditions, the same wind speed will generate less electricity in a warmer environment than in a colder one.

Relationship Between Climatic Variables and Their Impact on Wind Power Generation

The interactions between wind speed and temperature determine the performance of wind power installations under climate change scenarios. Specifically:

- If wind speed decreases and temperature increases, wind turbine efficiency could decline significantly.
- If wind speed increases but temperature also rises, the net effect will depend on which of the two factors has a greater impact on power generation.
- If wind speed remains stable but temperature increases, turbine efficiency could decrease due to lower air density, resulting in reduced electricity generation.

These factors highlight the importance of assessing climate projections through an integrated approach, considering not only changes in the mean values of climatic variables but also their distribution and variability over different time horizons.

6.3. Data Sources Used

To assess the impact of climate change on wind power generation, two main sources of climate data were used. First, reanalysis data were employed to characterize current climate conditions. Second, projections from regional climate models were used to estimate the future evolution of key climatic variables.

Reference Period 1991–2020 (ERA5)

The reference climate data were obtained from the ERA5 reanalysis dataset, as described previously. The extracted variables include air temperature at 2 meters (*2m_temperature*), expressed in Kelvin and subsequently converted to degrees Celsius, and wind speed at 10 meters, calculated from the zonal (*10m_u_component_of_wind*) and meridional (*10m_v_component_of_wind*) wind components, with values expressed in meters per second (m/s).

Regional Climate Model Projections to Estimate the Future Evolution of Climatic Variables (CORDEX)

To assess the future evolution of these variables under different climate change scenarios, projections from the Coordinated Regional Climate Downscaling Experiment (CORDEX), previously described, were used specifically for the South American domain.

6.4. Assessment of Climate Change Impacts on Wind Power Generation

Calculation of Wind Power Generation Potential

Wind power generation potential was calculated following widely used methodologies that make it possible to assess the impact of climate change on wind power generation by combining key climatic variables, such as wind speed and air temperature.

The performance of a wind turbine depends primarily on wind speed at rotor hub height. However, climate models generally provide near-surface wind speeds (typically at a height of 10

meters). To estimate wind speed at the operating height of the turbines (usually 80 meters), the wind shear equation is applied (Stadler et al., 2015):

$$U(t) = U_R(t) * \left(\frac{Z}{Z_R}\right)^{\alpha}$$

where:

- $U(t)$ is the estimated wind speed at rotor hub height (80 meters).
- $U_R\ (t)$ is the near-surface wind speed (10 meters).
- Z/Z_R is the ratio between the target height (Z) and the reference height.
- α is the wind shear exponent, which reflects atmospheric stability and varies with terrain roughness. This exponent is typically set to 1/7 under neutral atmospheric stability conditions, although it may be affected by climate change and changes in land use (Karnauskas et al., 2018; Tobin et al., 2016).

In addition to wind speed, air temperature plays an important role in turbine efficiency due to its effect on air density. The power extracted by a wind turbine is adjusted to account for air density using the following equation (based on Soubes et al., 2018):

$$Potencia = Potencia(v) * \left(\frac{15 + 273.15}{TAS + 273.15}\right)^{1/3}$$

where:

- $Potencia$ is the final power output adjusted for temperature.
- $Potencia(v)$ is the power output determined from the turbine's power curve.
- TAS is the near-surface air temperature.

This adjustment makes it possible to assess how projected temperature increases under different climate scenarios may affect wind power generation[5].

The relationship between wind speed and the power output of a wind turbine follows a characteristic power curve. At low wind speeds, power generation is zero or negligible, while maximum power output is reached at the rated wind speed. Above a certain threshold, turbines shut down to prevent structural damage. The following figure illustrates the selected power curve for a representative wind turbine:

Figure 6. Power Curve Values for a Representative Wind Turbine

[5] This procedure for estimating wind speeds at higher altitudes from near-surface reanalysis data could be improved if observational data at different heights were available, such as those provided by a wind profiler.

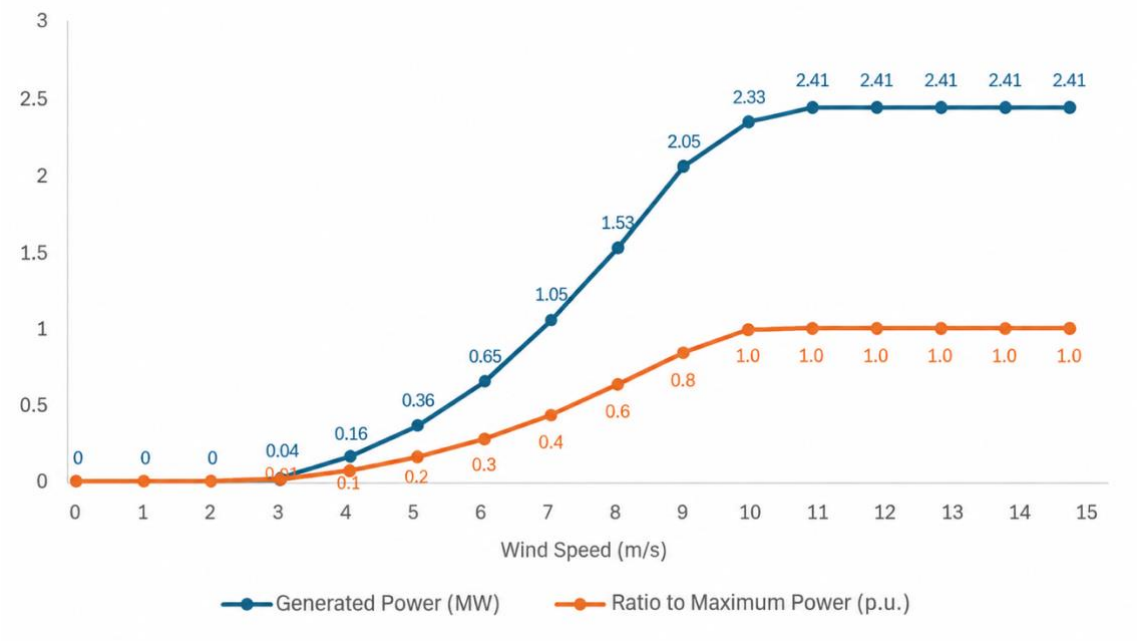

7. ASSESSMENT OF CLIMATE CHANGE IMPACTS ON TRANSMISSION AND DISTRIBUTION NETWORKS

7.1. Characterization of Climate-Related Hazards to Transmission and Distribution (T&D) Systems

The proposed methodological approach follows the recommendations of the Intergovernmental Panel on Climate Change (IPCC), according to which climate risk is defined by the interaction between climate-related hazards or threats, the exposure of systems to these hazards, and their vulnerability[6].

For overhead electricity transmission lines, the two most significant hazards are projected changes in ambient temperature and wind patterns, as both directly affect their ability to dissipate heat, with implications for their operation (i.e., their electricity transmission capacity) due to increased conductor resistance.

A more detailed description of this approach and the methodology used for its development is provided below.

Vulnerability of the Electricity Grid

The electricity grid is particularly vulnerable to changes in ambient temperature [7]. In the case of transmission lines, their safe operating range is reduced under high ambient temperature conditions, as their ability to dissipate the heat generated during operation (Joule heating) is diminished. This heat dissipation depends on the temperature difference between the conductor

[6] IPCC Sixth Assessment Report: Impacts, Adaptation and Vulnerability https://www.ipcc.ch/report/ar6/wg2/

[7] Allen-Dumas, Melissa R. Binita KC y Colin I Cunliff (2019). Extreme Weather and Climate Vulnerabilities of the Electric Grid: A Summary of Environmental Sensitivity Quantification Methods. https://www.energy.gov/sites/prod/files/2019/09/f67/Oak%20Ridge%20National%20Laboratory%20EIS%20Response.pdf

surface during operation and the external environment. Consequently, persistent high temperatures reduce heat dissipation, increasing conductor temperature and, in turn, its electrical resistance. This results in higher transmission losses and reduced electricity transmission capacity. If the conductor's maximum operating temperature is exceeded, overheating could cause physical damage to the infrastructure and increase the risk of fire. To prevent overheating that could compromise the physical integrity of the installation, the grid operator may choose to limit the maximum current carried by the line to maintain the conductor temperature at its design limit[8]. This requires reducing the maximum power that the line can transmit relative to its design conditions, thereby reducing operational efficiency. This is the approach adopted in this study.

The maximum current that a conductor can continuously carry without experiencing deterioration is limited by several factors: the conductor's structure and design (cable configuration, temperature rating, etc.), surrounding environmental conditions (ambient temperature, solar radiation, wind, etc.), and line operating conditions (line loading, type of installation, etc.). It is therefore a dynamic parameter that has traditionally been treated as a static value in design calculations, assuming the most adverse operating conditions based on historical climate data and adopting lower capacity limits to maintain adequate safety margins under all operating conditions.

However, under climate change, the design conditions originally assumed may no longer reflect future conditions, potentially limiting the line's ability to provide the service for which it was designed.

Figure 7. Comparison Between Static and Dynamic Maximum Current Ratings[9]

[8] Sathaye, Jayant, Larry Dale, Gary Fitts, Peter Larsen, Kevin Koy, Sarah Lewis, and Andre Lucena (2011). Estimating Risk to California Energy Infrastructure from Projected Climate Change. California Energy Commission. Publication number: CEC-500-2011-XXX. Availabe online: https://www.osti.gov/servlets/purl/1026811

[9] IRENA (2020), Innovation landscape brief: Dynamic line rating, International Renewable Energy Agency, Abu Dhabi. ISBN 978-92-9260-182-9

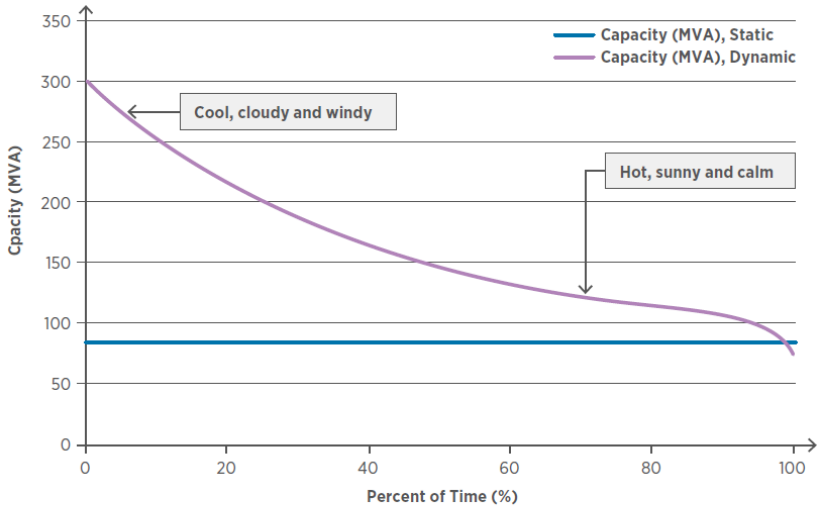

Note: MVA = megavolt ampere.
Source: Based on ENTSO-E (2015).

Figure 12 illustrates how the capacity of a transmission or distribution line can vary depending on climatic conditions and the methods used to calculate its capacity. The straight blue line represents the capacity rating that would be adopted if dynamic adjustments based on environmental conditions were not possible. This is the methodology generally employed, whereby a conservative, constant maximum capacity rating is established for periods spanning several weeks. The purple curve represents the capacity rating that could be calculated using *Dynamic Line Rating* (DLR). It illustrates the maximum capacity that could be utilized if the line's capacity were continuously adjusted according to forecast conditions for the coming hours. The figure shows that, in the absence of DLR, conservative decisions are made regarding the transmission capacity of power lines. Consequently, even slight increases in temperature may lead operators to continuously operate the infrastructure at a reduced capacity.

Different approaches can be used for this calculation. The most widely known algorithms are those developed by IEEE[10] and CIGRE[11], which use detailed information on the physical properties of the conductor and atmospheric conditions as inputs. However, most existing algorithms introduce uncertainties that can be substantial, particularly when line loading causes the conductor temperature to approach its maximum allowable limit. Furthermore, the algorithms must be adapted to the specific conditions and implementation practices of grid operators. Therefore, in addition to developing a robust calculation algorithm, a large amount of input data is required.

Given the difficulty of applying these types of algorithms within the scope of this study due to the lack of detailed information on the infrastructure, a simplified methodology is proposed. This approach, while adhering to relevant scientific recommendations, enables a quantitative assessment using the data currently available.

[10] IEEE Standard 738-2012, "IEEE Standard for Calculating the Current-Temperature Relationship of Bare Overhead Conductors", 2012.

[11] CIGRE Technical Brochure 207, "Thermal Behaviour of Overhead Conductors, Working Group 22.12", 2002.

7.2. Methodological Approach to Climate Risk Assessment

This study is based on the raster layers generated for **overhead transmission and distribution (T&D) lines**, which illustrate the impact of projected changes in ambient temperature and wind patterns on their operation (electricity transmission capacity). The two Essential Climate Variables (ECVs) considered are the Absolute Change in Ambient Temperature and the Absolute Change in Wind Speed, applied as shown in Table 4.

Table 3 Excerpt from the Table Relating Energy Infrastructure Components to Threshold Values and Potential Impacts.

ECV	Element	Material	
		Aluminium / Copper	Other / Unkown
Absolute Change in Ambient Temperature	Overhead Power Line	For every 1°C increase above 20°C, the amount of electricity transmitted decreases by 0.4%	For every 1°C increase above 20°C, the amount of electricity transmitted decreases by 0.3%.
Absolute Change in Wind Speed	Overhead Power Line	For every 1 m/s increase in average wind speed, electricity transmission capacity increases by 20%	

Source: screEN-LAC Project

According to Table 4, the specific approach used to assess the **impact of changes in ambient temperature** is based on applying a correction coefficient to the design maximum allowable current rating (assuming an ambient temperature threshold of 20°C) to determine the maximum allowable current at other temperatures. The correction coefficient was selected based on the conductor characteristics and ambient temperature and was applied whenever the ambient temperature exceeded 20°C.

Similarly, the **impact of changes in wind speed** is assessed by applying a correction coefficient that adjusts the electricity transmission capacity of power lines according to changes in wind speed, which helps cool the conductors.

Thus, the resulting impact represents the change in transmission capacity relative to the historical baseline under the different future scenarios analyzed. The ranges considered express this change as a percentage, with a positive or negative sign indicating an increase or decrease in capacity, respectively.

8. ASSESSMENT OF CLIMATE CHANGE IMPACTS ON COASTAL FACILITIES

8.1. Characterization of Climate-Related Hazards to Wind Power Systems

Among the facilities assessed under the screEN-LAC II project were two energy facilities located along the coast. Given that these facilities were designed to meet high resilience standards against natural hazards, the study focused specifically on the potential impacts of sea level rise. Unlike other climate-related hazards with more immediate effects, sea level rise is a gradual and cumulative process that may pose a significant risk to strategic coastal infrastructure over long-term time horizons.

The limitations in the site-specific information available for both facilities, together with the possibility of consistently applying the same observational datasets and modeling results, led to the adoption of a joint analysis. This approach makes it possible to optimize the use of available information and ensure consistent criteria for risk assessment, the results of which are presented in this document.

8.2. Concepts Related to Sea Level Height

Sea level in a coastal area results from the interaction of various physical processes operating on different timescales. These include astronomical tides, caused by the gravitational attraction of the Moon and the Sun; meteorological tides, associated with wind and atmospheric pressure variations during storms and hurricanes; climatic and oceanographic variability; and the rising trend in mean sea level associated with climate change.

Measurements obtained from ocean buoys and tide gauges primarily represent the elevation of the sea surface under still-water conditions (Still Water Level), without accounting for the local effects of wave transformation as waves approach the coast. In these areas, decreasing water depth causes changes in wave characteristics and wave breaking, resulting in an additional increase in mean water level known as wave setup. Similarly, the temporary uprush of water caused by each individual wave onto beaches and coastal structures is known as wave run-up. These phenomena can significantly increase the maximum water level reached compared with that recorded offshore.

The study aims to assess the evolution of the hazard associated with sea level rise using data from buoys, tide gauges, and oceanographic products derived from observations and numerical models. Accordingly, its results describe the expected evolution of sea level and its components, without accounting for the specific effects of coastal wave transformation, which require specialized hydrodynamic and engineering studies.

Finally, rising mean sea level raises the baseline upon which these processes act, potentially increasing the frequency and magnitude of coastal flooding over the long term.

8.3. Assessment of the Impacts of Sea Level Rise

The objective of this analysis is to estimate extreme sea levels at two coastal facilities located along the shoreline and assess how their frequency of occurrence will change as a result of climate change-induced mean sea level rise. Sea levels corresponding to return periods of 10 and 100 years (T10 and T100) are examined for the 2030, 2050, and 2100 time horizons under the SSP1-2.6, SSP2-4.5, and SSP5-8.5 emissions scenarios defined by the IPCC. The wave regime is also characterized to provide context for extreme marine conditions.

The methodology combines observations from a tide gauge and a buoy in Juan Dolio with historical reconstructions obtained from numerical models covering approximately 75 years. These time series incorporate IPCC sea level rise projections and specific datasets representing storm surges associated with tropical cyclones and hurricanes, enabling the estimation of present and future extreme sea levels.

The results represent the still water level offshore of the facilities, accounting for mean sea level, astronomical tides, and meteorological tides. They do not include local wave transformation

effects, such as wave setup, wave run-up, and overtopping of coastal structures, due to the lack of detailed information on existing coastal defenses.

Finally, elevations are expressed relative to the mean sea level recorded during 2023–2024. Therefore, they do not represent absolute topographic elevations and cannot be directly compared with the elevations of the facilities without precise vertical datum alignment between the tidal datum and the corresponding elevation reference systems.

8.4. Data Used in the Analysis

The assessment of marine hazards affecting coastal facilities is based on the integration of local observations, reanalysis datasets, historical reconstructions, and climate projections. This combination makes it possible to reconstruct approximately 75 years of marine variability, characterize mean and extreme sea level conditions, and assess their future evolution under different climate change scenarios.

Local observations are obtained from a tide gauge and an oceanographic buoy that provides wave data. Although these time series are too limited for a robust statistical analysis of extreme events, they make it possible to validate regional datasets and characterize recent marine conditions.

The historical reconstruction uses the GTSM v3.0 hydrodynamic model, forced by ERA5, which provides hourly data on total sea level and meteorological tide residuals from 1950 onward. The ERA5 reanalysis is also used to obtain wave variables, such as significant wave height, wave period, and wave direction. The evolution of mean sea level is cross-checked against the DUACS multi-mission satellite altimetry product, available since 1993.

To assess the future effects of climate change, regional projections from the IPCC AR6 are incorporated under the SSP1-2.6, SSP2-4.5, and SSP5-8.5 scenarios, considering the 2030, 2050, and 2100 time horizons. In addition, the COAST-RP product enables the estimation of extreme sea levels associated with return periods of up to 1,000 years, using historical storms and synthetic tropical cyclones.

An important limitation is the lack of permanent monitoring sensors and site-specific hydrodynamic models for each facility. Therefore, some regional datasets are considered representative of both locations, without fully capturing local differences in bathymetry, coastal orientation, and geomorphology. Consequently, the results provide a regional characterization of marine hazards and should be interpreted in light of these limitations.

For another coastal facility included in the study, the probability of occurrence of storms that could pose a threat to the plant's operability was assessed. The following methodology was applied for this analysis:

8.5. Methodology for Storm Characterization

The methodology is structured into five stages: storm characterization using Global Climate Models (GCMs), generation of a multimodel precipitation ensemble, development of frequency and cumulative probability curves, application of the Quantile Delta Mapping (QDM) method to incorporate the climate change signal, and analysis of projection uncertainty.

Storm characterization is carried out using three-hourly precipitation records. Each event is defined as a sequence of consecutive records with precipitation equal to or greater than 0.1 mm per three-hour interval and ends when a dry interval is recorded. This threshold makes it possible to exclude negligible precipitation or values associated with numerical noise in the models, while retaining more than 98% of annual precipitation. Three indicators are calculated for each storm: duration, expressed in hours; cumulative precipitation depth, obtained by summing the recorded precipitation; and mean intensity, calculated as the ratio of cumulative precipitation depth to storm duration.

The ensemble is constructed from four CMIP6 climate models by averaging their quantile distribution functions rather than directly averaging the time series. For each probability level, the corresponding precipitation depth is calculated for each model, and the mean of these values is obtained. This procedure makes it possible to integrate the statistical distributions of the models and provide a combined representation of precipitation behavior.

Subsequently, percentage frequency curves are developed to describe the proportion of storms falling within different cumulative precipitation depth intervals. These are then used to generate cumulative probability curves, which indicate the percentage of events with precipitation depths less than or equal to a given value. The seven observed storms are treated as classes within a grouped frequency distribution, with each interval assigned the cumulative probability corresponding to its midpoint, without assuming that the highest observed value represents the maximum possible precipitation depth.

Finally, the QDM method is used to transfer the climate change signal from the models to the observed historical distribution. Its application is appropriate given the differences between simulated storms and those recorded at La Teja, particularly in terms of duration and intensity. These discrepancies are partly attributable to differences in spatial and temporal resolution between global models, which represent averages over grid cells of approximately 100 km, and higher-resolution point observations. Therefore, the objective is to incorporate projected climate changes without attempting to artificially reproduce all the characteristics of the observed storms. The uncertainty analysis complements this procedure and makes it possible to assess the variability of future results.

9. GENERAL CONCLUSIONS ON THE METHODOLOGIES APPLIED IN THE STUDY:

Depending on the type of energy facility assessed, analytical methodologies were applied based on the selection of climate and socioeconomic scenarios, as well as global and regional circulation models. These approaches enabled plausible projections of the future behavior of Essential Climate Variables (ECVs) that characterize the potential hazards, impacts, and risks associated with climate change to which the energy sector infrastructure included in the study across the five beneficiary countries may be exposed.

The methodologies, procedures, and calculations applied do not yield single values, but rather ranges of values derived from combinations of scenarios, models, ensembles, and simulation periods. The mean values within these ranges are selected and presented as the results of each analysis.

The quality and accuracy of the results obtained from the various simulations depend on the historical information available for each facility assessed. Therefore, it is important to maintain

systems for monitoring the climatic conditions under which these facilities operate, including, depending on the type of facility, inflow rates, solar radiation, wind speed, ambient temperature, sea level, and the intensity and frequency of extreme events, among other variables.

10. REFERENCES

1. Cannon, A. J., S. R. Sobie, T. Q. Murdock, 2015. Bias Correction of GCM Precipitation by Quantile Mapping: How Well Do Methods Preserve Changes in Quantiles and Extremes?. J. Climate, 28, 6938–6959, https://doi.org/10.1175/JCLI-D-14-00754.1.
2. Chenni, R., Makhlouf, M., Kerbache, T. & Bouzid, A., 2007. A detailed modeling method for photovoltaic cells. Energy 32, 1724–1730 (2007). DOI: 10.1016/j.energy.2006.12.006.
3. Crook, J. A. 2011. Climate change impacts on future photovoltaic and concentrated solar power energy output. http://dx.doi.org/10.1039/C1EE01495A.
4. Energías Renovables. 2015. The Effects of Temperature on Power Generation in Photovoltaic Installations. Available at: https://www.energias-renovables.com/fotovoltaica/los-efectos-de-la-temperatura-en-la-20150713.
5. Jerez, S., Tobin, I., Vautard, R., Montávez, J.P., López-Romero, J.M., Thais, F., Bartok, B., Christensen, O.B., Colette, A., Déqué, M., Nikulin, G., Kotlarski, S., van Meijgaard, E., Teichmann, C., Wild, M., 2015. The impact of climate change on photovoltaic power generation in Europe. Nat Commun 6, 10014. https://doi.org/10.1038/ncomms10014.
6. Iglewicz, B. & Hoaglin, D. C., 1993. How to detect and handle outliers (Vol. 16). ASQC Quality Press.
7. Park, C., Cha, D.-H., Shin, S.-W., Kim, G., Kim, T., 2020. Future projections of photovoltaic power generation on climate change simulated by CORDEX II multi-RCMs over East Asia (No. EGU2020-12934). Copernicus Meetings. https://doi.org/10.5194/egusphere-egu2020-12934.
8. Karnauskas KB, Lundquist JK, Zhang L. Southward shift of the global wind energy resource under high carbon dioxide emissions. Nature Geosci. 2018;11(1):38-43. DOI: 10.1038/s41561-017-0029-9.
9. Tobin I, Jerez S, Vautard R, et al. Climate change impacts on the power generation potential of a European mid-century wind farms scenario. Environ Res Lett. 2016;11(3):034013. DOI: 10.1088/1748-9326/11/3/034013.
10. Pablo Soubes, Felipe Palacio, Ruben Chaer. 2018. Wind Power Plant Model. Electricity Market Administration (ADME). https://www.adme.com.uy/db-docs/Docs_secciones/nid_324/ModeloCentralGeneradoraEolica.pdf.
11. Stadler, Stephen, James M. Dryden Jr., and J. S. Greene. 2015. "Climate Change Impacts on Oklahoma Wind Resources: Potential Energy Output Changes" Resources 4, no. 2: 203-226. https://doi.org/10.3390/resources4020203.
12. Karnauskas KB, Lundquist JK, Zhang L. Southward shift of the global wind energy resource under high carbon dioxide emissions. Nature Geosci. 2018;11(1):38-43. DOI: 10.1038/s41561-017-0029-9
13. Tobin I, Jerez S, Vautard R, et al. Climate change impacts on the power generation potential of a European mid-century wind farms scenario. Environ Res Lett. 2016;11(3):034013. DOI: 10.1088/1748-9326/11/3/034013

14. Pablo Soubes, Felipe Palacio, Ruben Chaer. 2018. Wind Power Plant Model. Electricity Market Administration (ADME). https://www.adme.com.uy/db-docs/Docs_secciones/nid_324/ModeloCentralGeneradoraEolica.pdf

15. Stadler, Stephen, James M. Dryden Jr., and J. S. Greene. 2015. "Climate Change Impacts on Oklahoma Wind Resources: Potential Energy Output Changes" Resources 4, no. 2: 203-226. https://doi.org/10.3390/resources4020203



@olacde

olacde.org